Supplemental Material

Earth Interactions
https://doi.org/10.1175/EI-D-21-0004.1

Space-Time Variability of Summer Hydroclimate in the United States Prairie Pothole Region

Benjamin D. Abel[1], Balaji Rajagopalan[1,2], Andrea J. Ray[3]

[1] Department of Civil, Environmental, and Architectural Engineering, University of Colorado Boulder, Boulder, CO, United States of America
[2] Cooperative Institute for Research in Environmental Sciences, University of Colorado Boulder, Boulder, CO, United States of America
[3] National Oceanic and Atmospheric Administration, Physical Sciences Laboratory, Boulder, CO, United States of America

E-mail: benjamin.abel@colorado.edu

Supplementary Material

PCA of Summer Average Precipitation – Scree Plot

To choose the number of PCs to retain for analysis, we used the common method sometimes called the "elbow test". First, one searches for the place on a scree plot (Cattell 1966) where the slope goes from large to small, often called an "elbow" (Jolliffe 2002). Then, the components to the left of the elbow are retained. The scree plot of the eigenvalues from PCA performed the CD precipitation data averaged spatially by CD and temporally by summer is shown in Figure S1. There are two places the graph levels off (the "elbow"). The first is after PC2 – PC3 and PC4 have similar contributions to variance. There is a second drop after PC4. PC5 and higher all contribute very little to the data variance. We examined results from PC3, but no significant patterns or correlations were noticed. Therefore, we chose to use PC1 and PC2 for analysis.

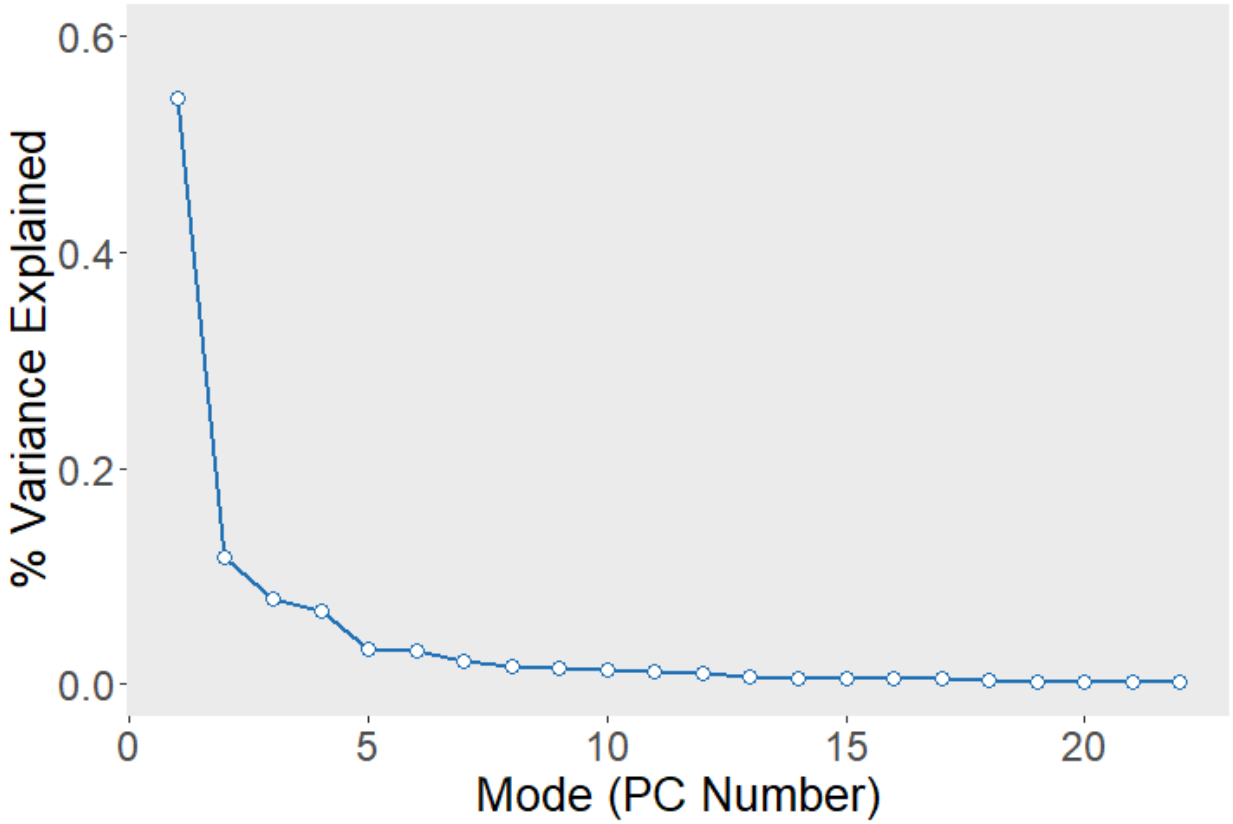

Figure S1: Scree plot of all 22 PCs from PCA on CD precipitation.

Large-Scale Climate Teleconnections – Regression Coefficients Significant at 95%

Figures S2 and S3 show a regression analysis performed in a similar manner to the correlation analysis outlined in section 3b and discussed in section 4c – a linear model has been fitted at each grid point, then the regression coefficient has been plotted. Significant regression coefficients (95%) have been outlined in the plots.

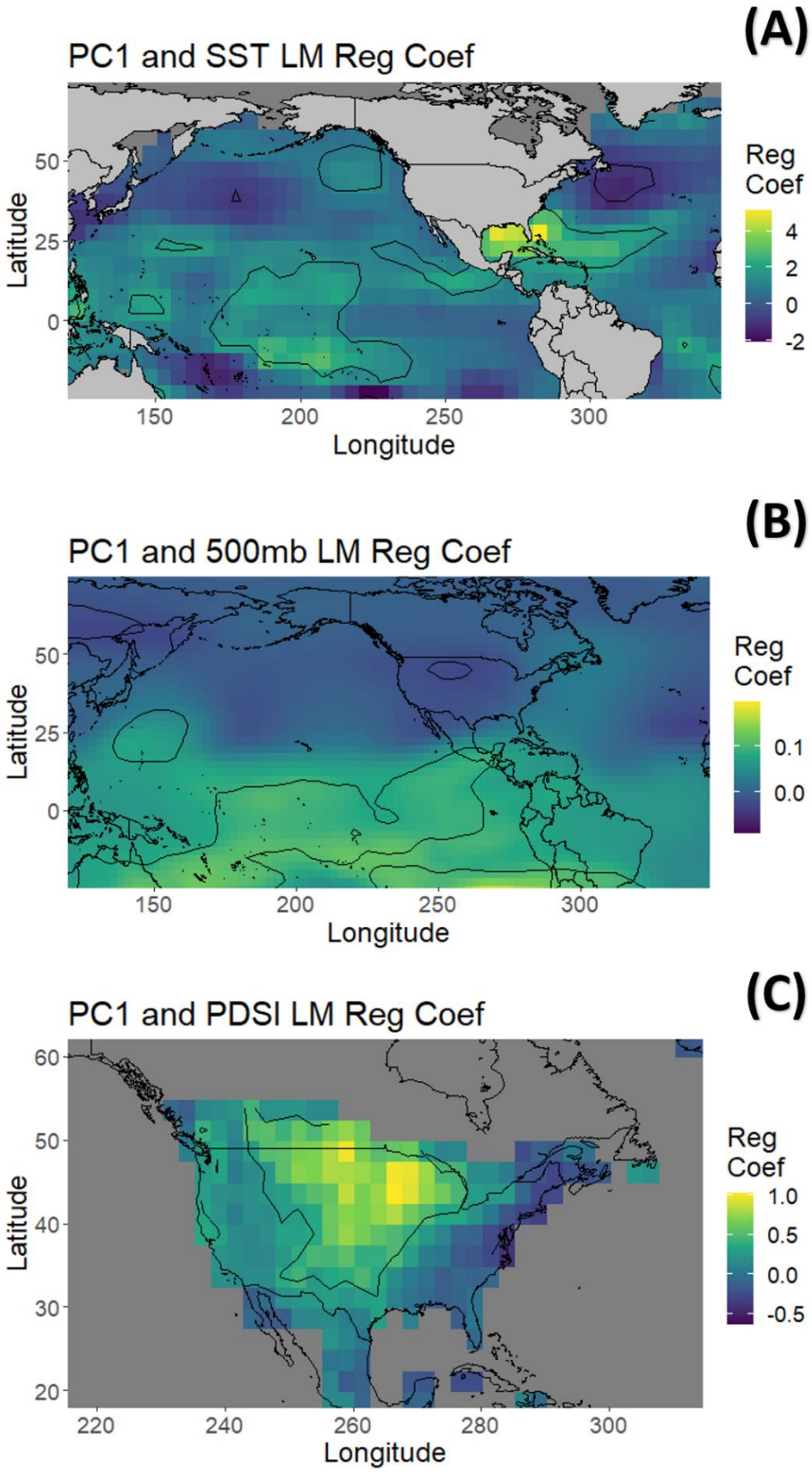

Figure S2: Regression coefficient of the linear model at each grid point of PC1 with (A) SST anomalies, (B) 500 mb heights, and (C) PDSI. Coefficients significant at the 95% level are enclosed in the contour.

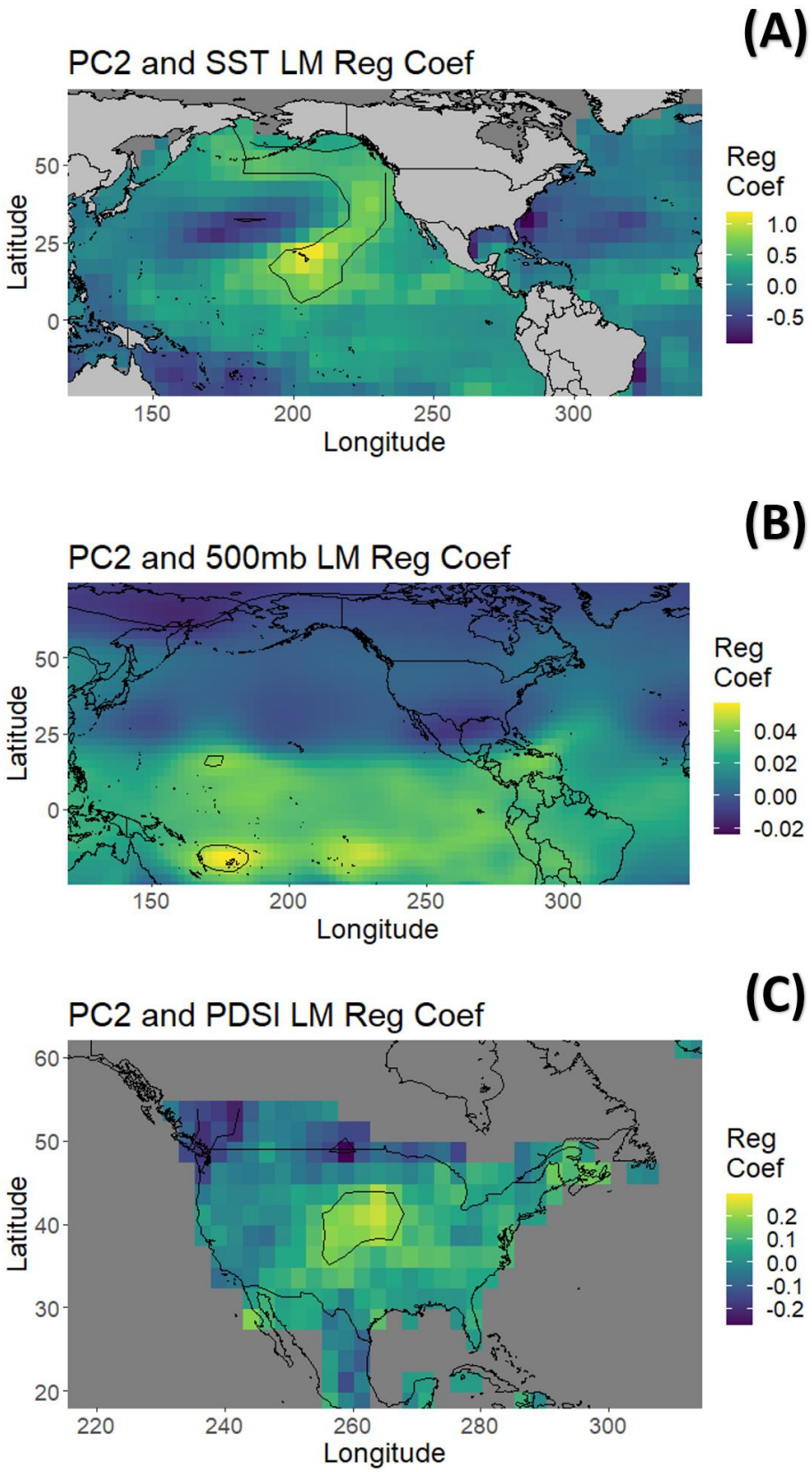

Figure S3: Regression coefficient of the linear model at each grid point of PC2 with (A) SST anomalies, (B) 500 mb heights, and (C) PDSI. Coefficients significant at the 95% level are enclosed in the contour.

Potential Mechanisms Driving Variability – PC2

Figures S4 and S5 show the composites of the extreme wet and dry years of PC2 (Table 2). The potential mechanisms elucidated by these results are present in the wet and dry analysis of PC1. There are anomalously low 500mb heights over the SEPPR for PC2 wet years (Figure S4 A). There are high PDSI anomalies to the southwest of the SEPPR for PC2 wet years (Figure S5 C). There are no other strong, prominent features in the remainder of the composite maps.

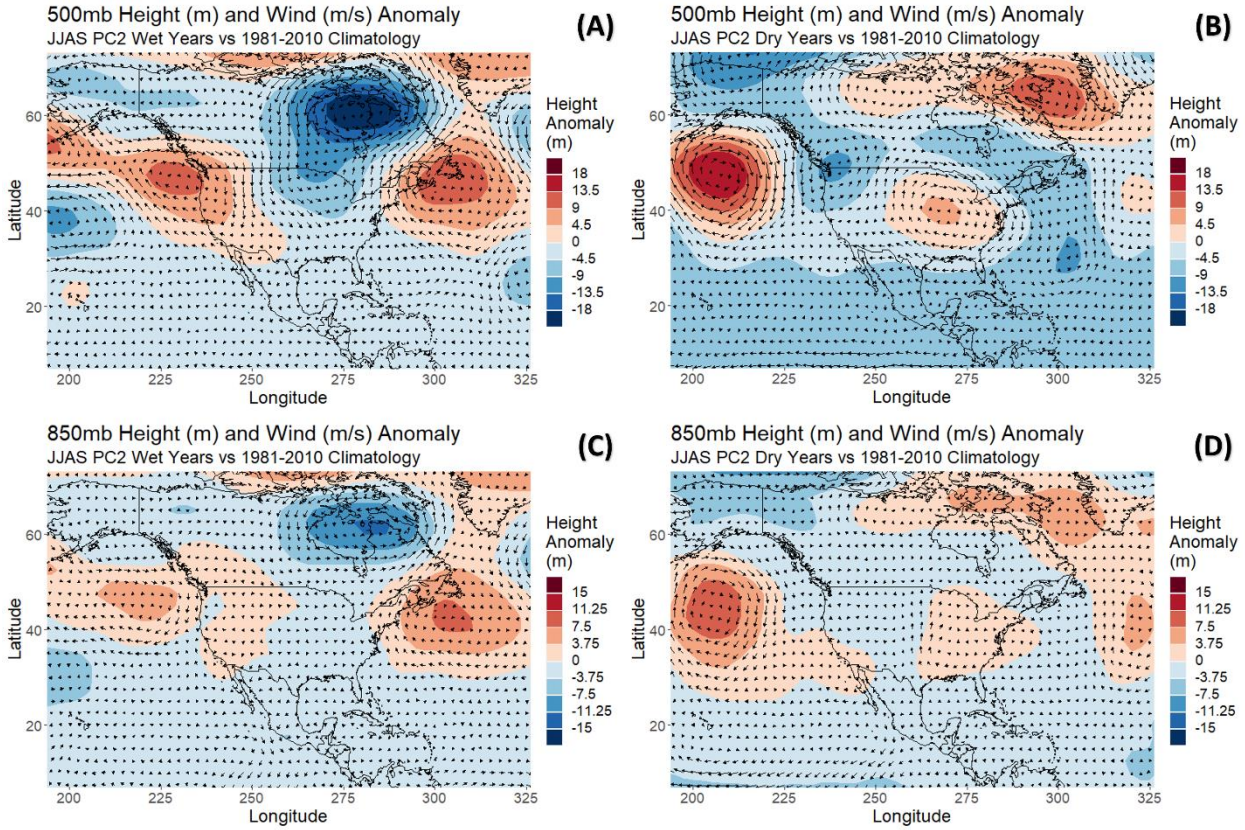

Figure S4: The same as Figure 7 but for PC2.

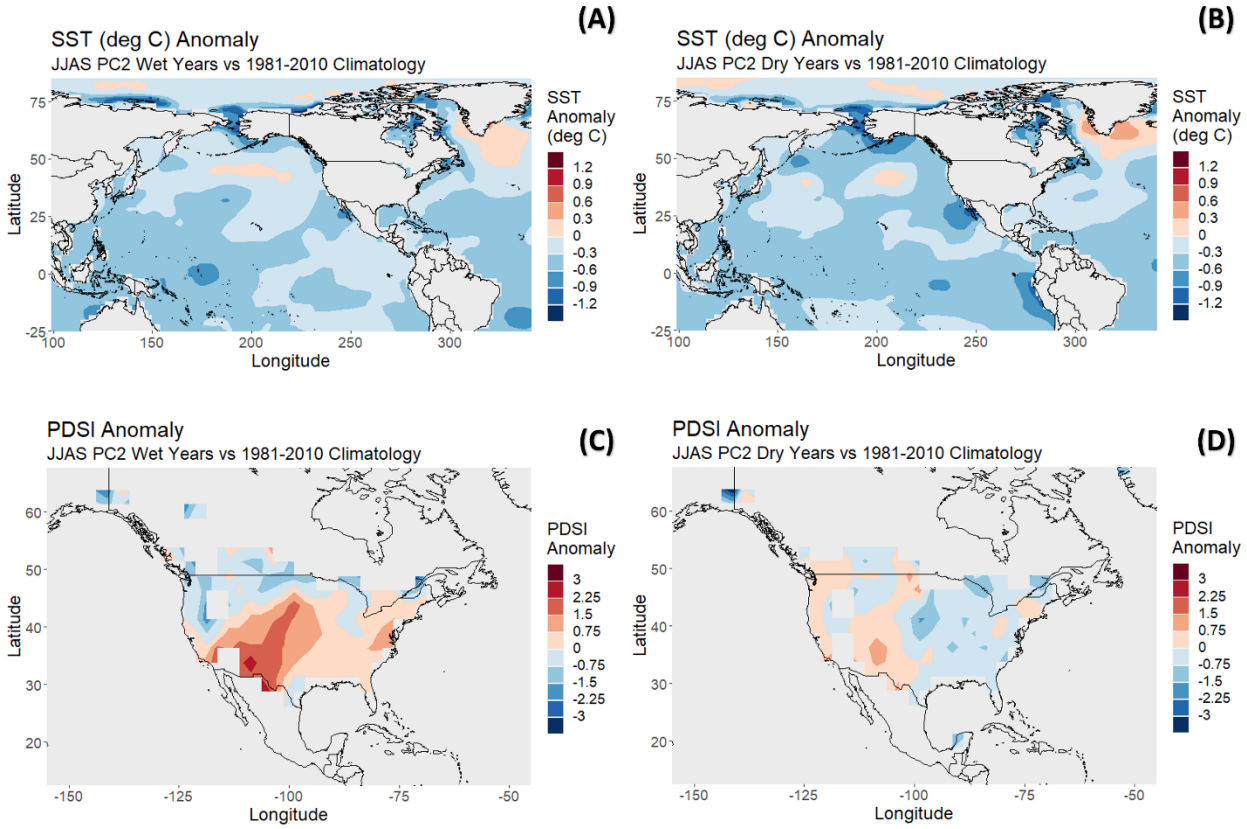

Figure S5: The same as Figure 8 but for PC2.

Potential Mechanisms Driving Variability – Precipitable Water and Soil Moisture

The extreme wet years of PC1 have positive anomalies of precipitable water over most of the GPLLJ region (Figure S6 A). Recall the GPLLJ brings moisture from the Gulf of Mexico northward to the Midwest. In addition, there are positive soil moisture anomalies in the SEPPR during these years (Figure S6 B). In contrast to the extreme wet years, the dry years of PC1 have negative anomalies of precipitable water and soil moisture over the SEPPR (Figure S7 A, S7 B). These results indicate the presence of increased moisture for summer precipitation during wet years and a lack of moisture for summer precipitation during dry years.

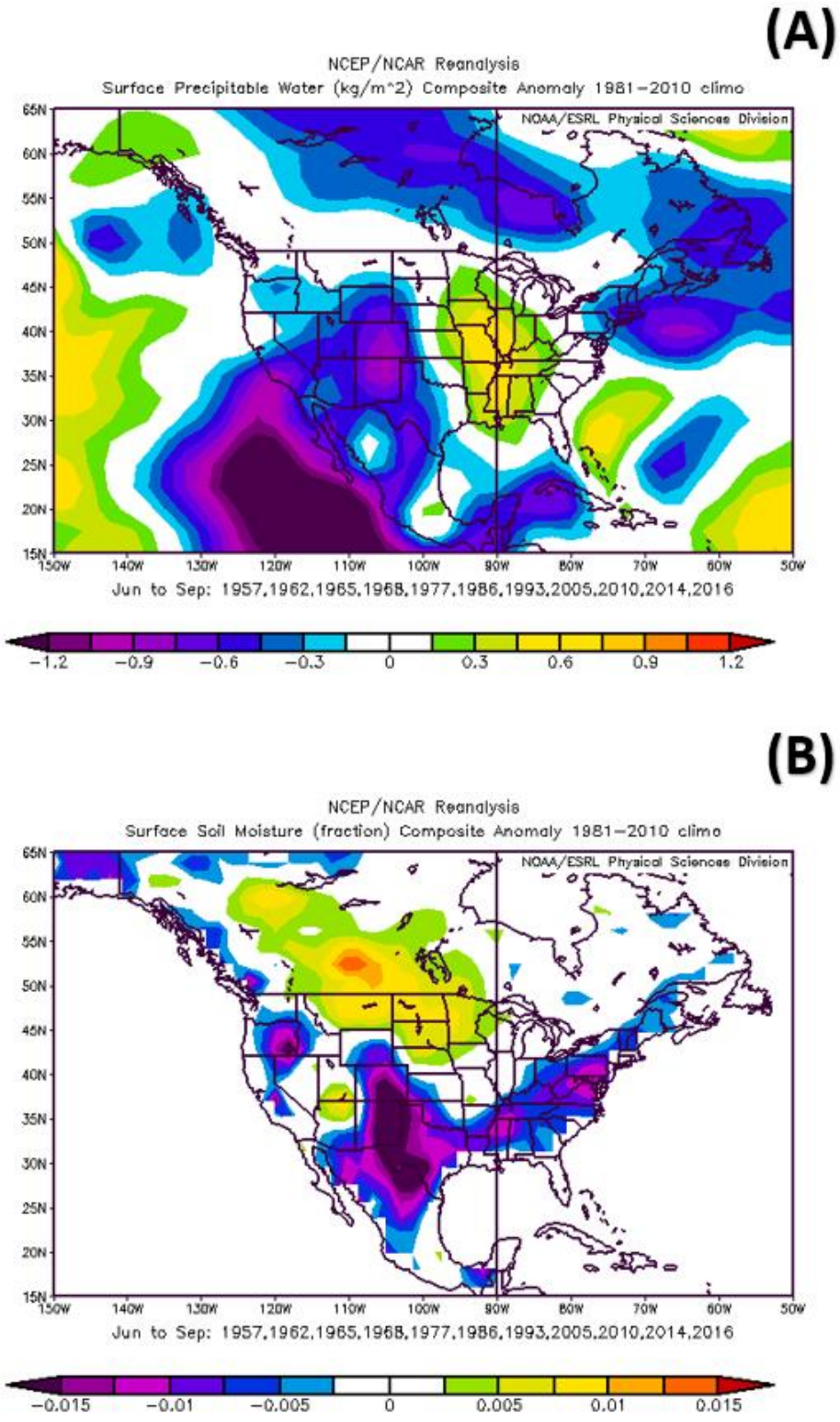

Figure S6: Summer composites of (A) precipitable water and (B) soil moisture for the wet years of PC1.

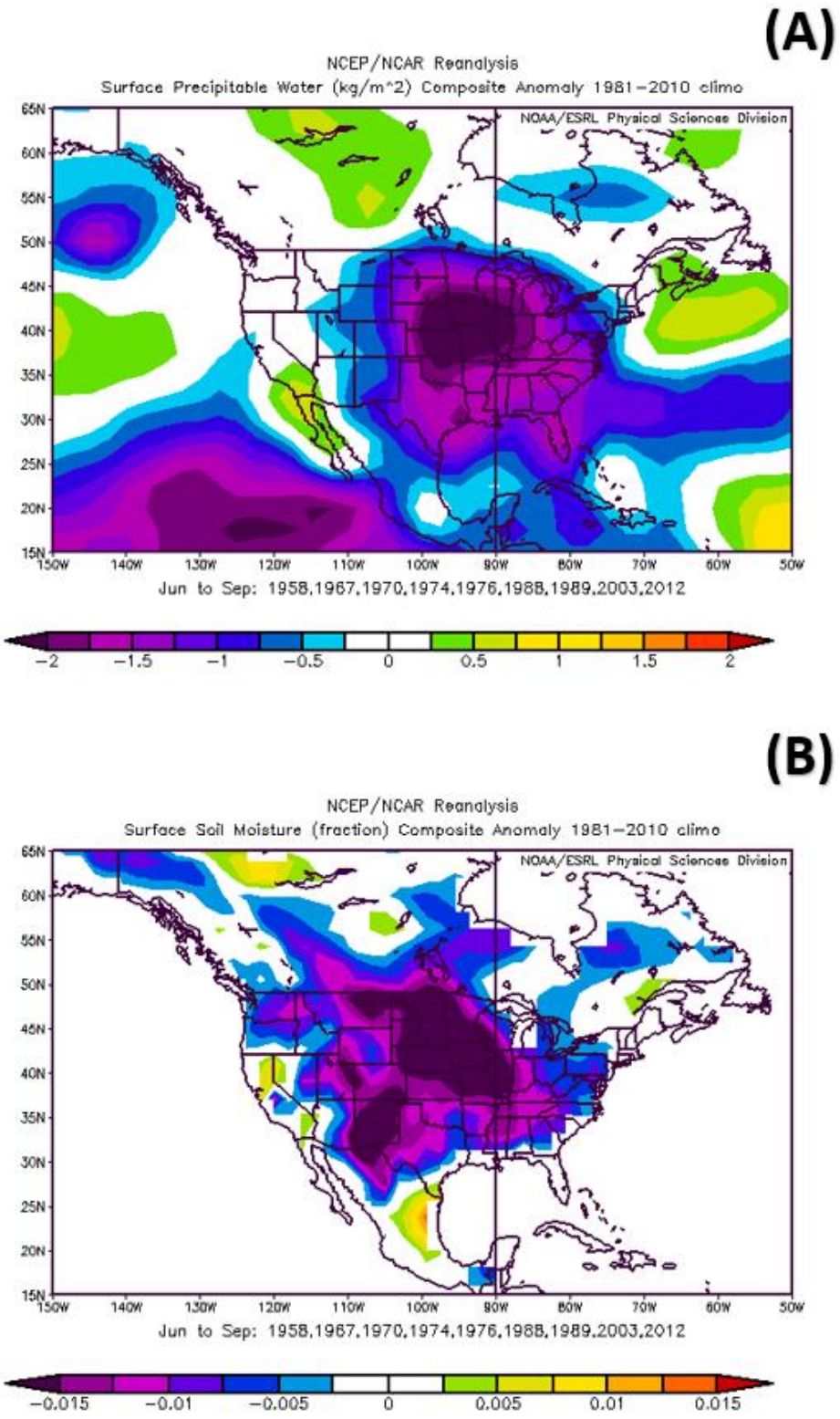

Figure S7: Summer composites of (A) precipitable water and (B) soil moisture for the dry years of PC1.

Wavelet Analysis

We performed wavelet analysis on PC1 (from PCA of summer precipitation), the summer-averaged Nino 4 index, and the summer-averaged PDO index as a diagnostic tool to further examine the connection between precipitation variability and SSTs. We used a continuous wavelet transform (CWT) using the Morlet wavelet for PC1 to produce the wavelet power spectrum (Figure S8). A wavelet coherence spectrum, essentially a measure of correlation between two individual CWTs, is generated for PC1 with both the Nino 4 index and PDO index (Figure S9). Further information on these techniques can be found in Torrence and Compo (1998).

The PC1 power spectrum displays appreciable power in the 2- to 4-year band throughout the entire time series, in the 4- to 8-year band from 1985 until the end, in the 8- to 16-year band from the beginning of the time series to 1925, and in the 16- to 32-year band from 1915-1965 (Figure S8).

In the coherence spectrum between PC1 and the summer-averaged Nino 4 index (Figure S9 A), there are numerous periods with significant coherence levels (significant at the 10% level). There are three in the 2- to 4-year band from 1965-1970, 1975-1980, and 2008-end of record. There is an extended time of significance from 1960-1980 in the 16-year period. There are also significant spans from 1950-1960 and 1980-1990 in the 8- to 16-year band.

The PC1 and the summer-averaged PDO index show the most significant time spans for the longer periods (Figure S9 B). These occur in the 8- to 16-year band from 1905-1945. From 1945-1975, there is a significant coherence with a period slightly longer than 16 years.

These wavelet analysis results reinforce connections seen in the main body of this work. PC1 has appreciable power in periods known to be common to both ENSO (~3-7 years) and PDO (~15-30 years). The coherence spectrums show regions of significance at the 10% level between PC1 and the two indices, also conveying that there is a teleconnection between the precipitation variability and these very common SST phenomena.

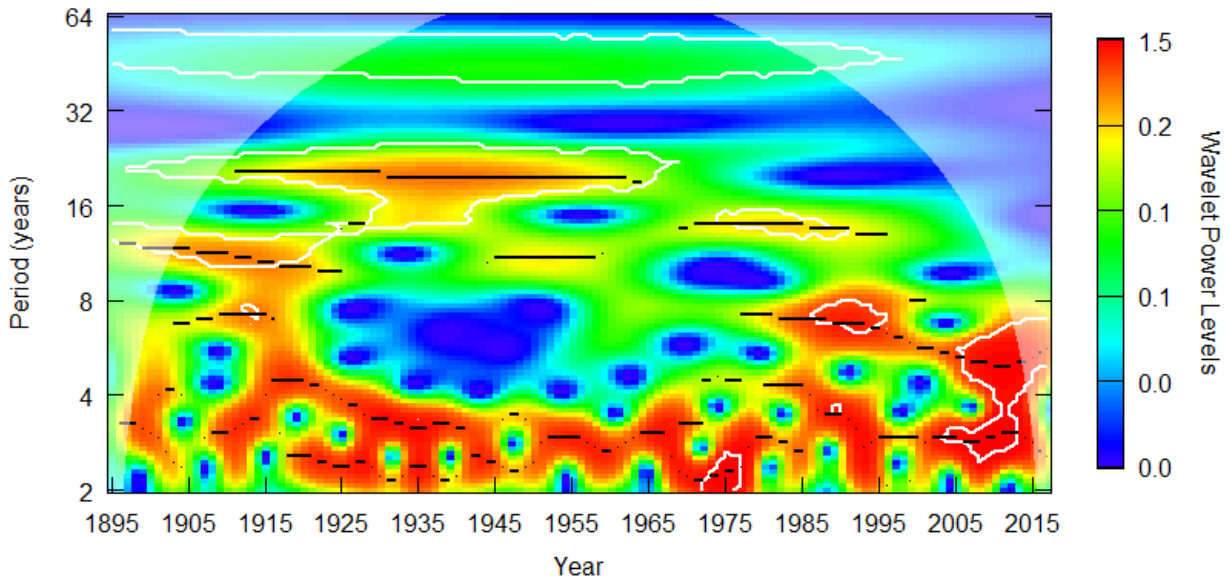

Figure S8: Wavelet power spectrum for PC1.

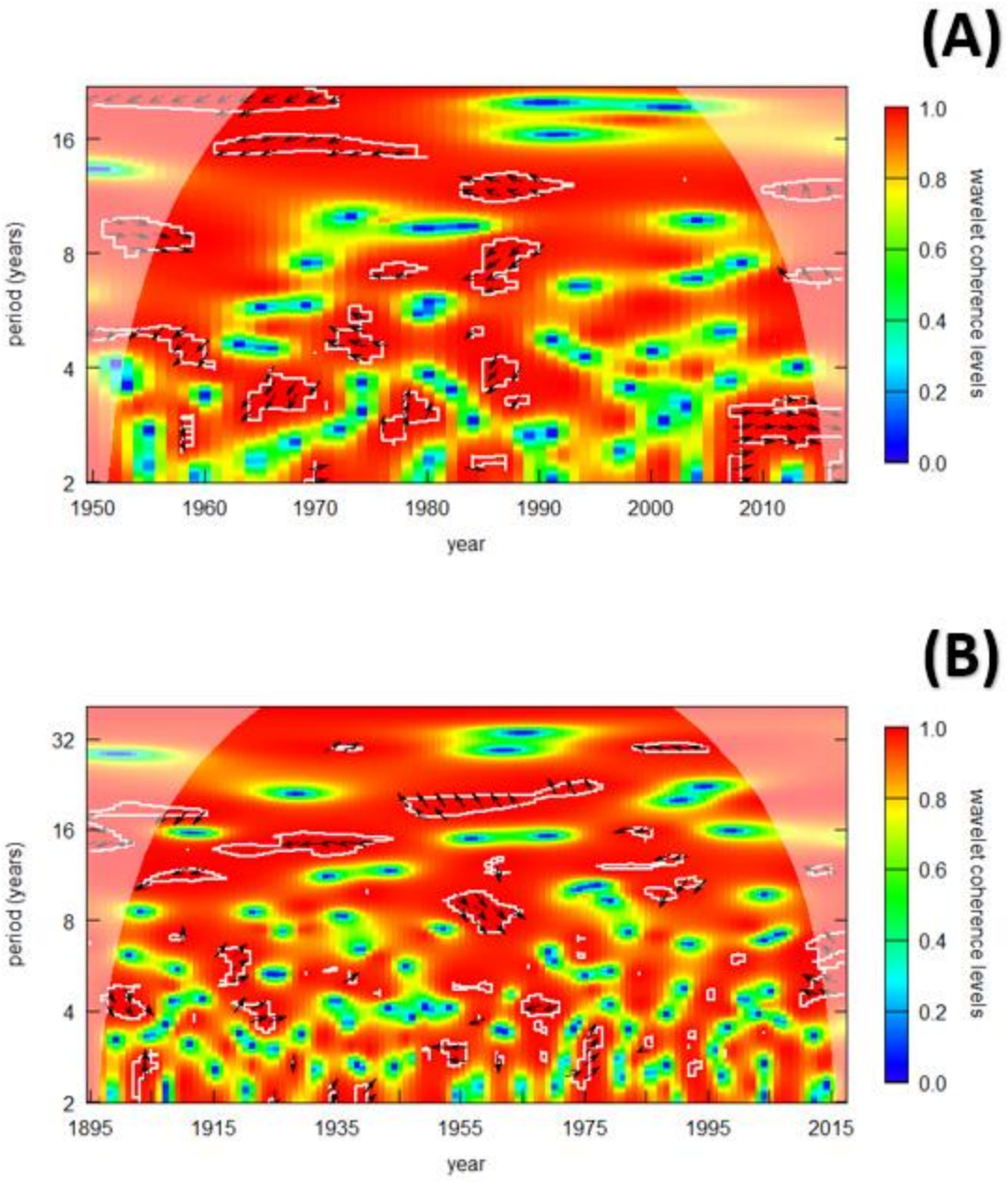

Figure S9: Wavelet coherence spectrums for (A) PC1 over Nino4 summer average and (B) PC1 over PDO summer average.